Design of Conformal Phased Array Architectures for Air Traffic Control Radars

P. Rocca, N. Anselmi, M. A. Hannan and A. Massa

Contents

1 Scope of the Document

Phased arrays are one of the most important technologies for the design of the newest antenna generations. This is true expecially in the field of radars for civil Air Traffic Control where old technologies such as reflector antennas are still widely used.

The first advantage of usign phased array is that it is possible to steer the beam without mechanical movements but only changing elements phases excitations in order to obtain a radiation that suits the given requirement.

Another advanage is that a phased array could be conformal to a particular structure so that the shape of the antenna could assume the same or very similar shape of its phisical support.

On the other hand, a conformal phased array could cost much more than a conventional reflector antenna system bacause it contains a large number of radiating elements that means huge number of electronic and microwave devices (phase shifter, amplifiers, Buttler matrices,etc), also in the case of digital beamforming network in which, instead of a phase shifter and an amplifier for each element, an analog to digital converter is required. High cost is the real deterrent that limits the realization of commercial devices based on phased array for civil applications. Hence a strategy to peform a consistent reduction of radiating elements is necessary to make the architecture proposed below attractive compared to real systems.

The aim of this work is the synthesis of a Conformal Phased Array Radar Architecture exploiting Multi-task Bayesian Compressive Sensing (*MT-BCS*). MT-BCS is an improvement of Bayesian Compressive Sensing that permits to deal with complex problems and not only with real ones as in case of BCS. In particular it is possible to solve a complex problem, such as array elements excitations synthesis, considering its real and imaginary parts not indipendent as in BCS but correlated by "shared-priors" that model the raltionship between them.

Proposed architecture is composed by a collection of sparse linear phased arrays arranged over a Truncated Cone structure. The shape of the structure has been choosen in order to exploit the slope of lateral surface and the circular symmetry of truncated cone geometry. In this way the radiation could be theoretically all around the antenna systems without mechanical rotating pedestal typical of commercial Airport Surveillance Radar achieving a sort of "ubiquitous " behavior.

MT-BCS has been applied on a reference Uniformly Spaced Linear Array to obtain a Sparse Linear Array that has been used then to compose the entire Truncated Cone Conformal Phased Array Radar Architecture.

At the end of the synthesis procedure has been obtained a sparse linear phased array with performances very similar to the non-sparse reference one, achieving a considerable saving on radiating elements.

The document contains the following parts. A description of the ATC Scenario is reported in *Section 2.1* with particular attention on Airport Surveillance Radar and precisely on Primary Surveillance Radar. In *Section 2.2* is presented the proposed architecture and in *Section 2.3* is reported a detailed conceptual and geometrical description of it. *Section 3* contains the mathematical formulation for the MT-BCS sparse linear array synthesis procedure and the computation of the error used to compare Reference and BCS array power pattern while in *Section 4* are reported power patterns of the USLA Reference array and the frequency analysis of power patterns of the Reference Truncated Cone structure. *Section 5* contains a first analysis on radiation using a

real dual band radiating element found in literature. Numerical Assesment, at *Section* 6, contains the results on MT-BCS sparse linear array synthesis, the frequency analysis of the Truncated Cone structure composed by sparse linear arrays and the comparison between Reference and BCS power patterns over the selected frequency range. Finally Comments in *Section 7* and Conlusion and Future Works in *Section* 8.

2 Problem Statement

2.1 Air Traffic Control Scenario

Surveillance systems in airport environments are vital for the correct execution of all terminal functions and procedures as take off and landing of airplanes, air traffic management and terminal secuirty procedures.

It is possible to define these systems as *Airport Surveillance Radar* (*ASR*). ASR are usually based on ground stations characterized by a large reflector or panel antennas placed on a mechanical structure that permits the rotation of the antenna system in order to scan the space all around it as shown in *Fig.1* and in *Fig.*2.
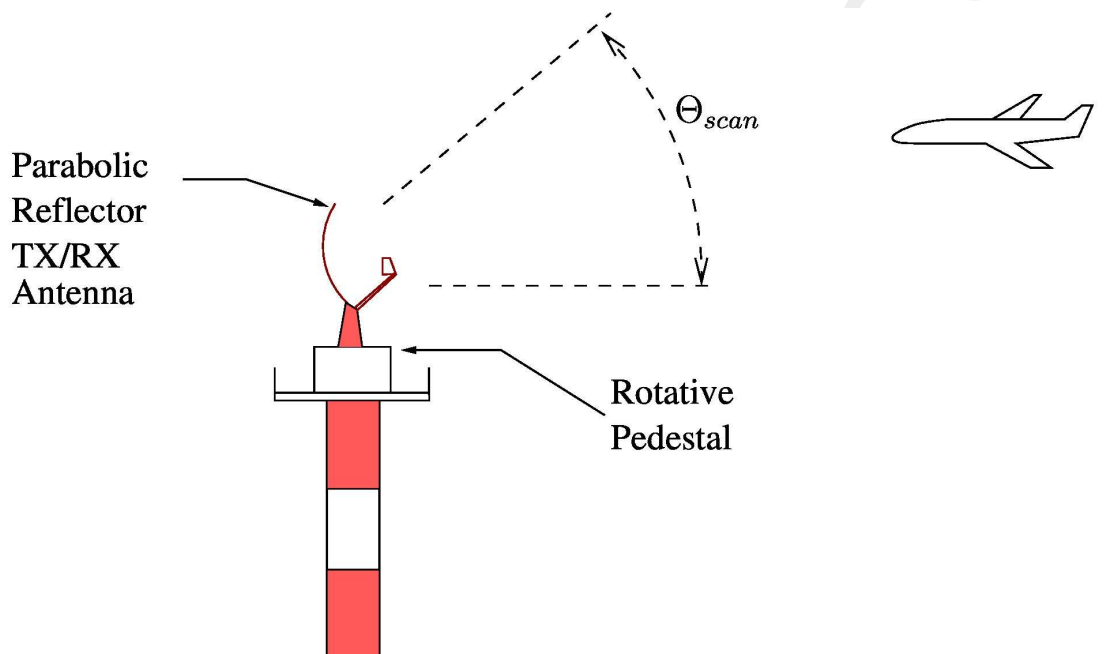
Figure 1: Actual Air Traffic Control scenario

ASRs are divided in PSR (Primary Surveillance Radar)(parabolic reflector in *Fig.*2) that detects and tracks the position of reflecting objects in the coverage area and SSR (Secondary Surveillance Radar)(*Fig.*2, the rectangular antenna placed above the PSR) that detects, tracks and identifies airplane by means of communication between the ground station and the aircraft transponder.

Figure 2: ELDIS RL-2000 PSR and SSR

Focusing on PSR, the scanning procedure is based on the transmission of a pulse and the reception of the returning echo backscattered by a reflecting object, that could be for example a plane. The beam pattern usually used in PSR systems is a cosecant square that permits the radar to illuminate the entire elevation range at the same time. It can be noticed that the radar covers with its radiation an angular range in elevation that is of about $\Theta_{scan} = 40$.

Figure 3: Indra PSR System

As compliant to Eurocontrol specifications, frequency bands reserved for aeronautical radionavigation and radiolocalization and in particular for PSR applications are two:

- L-band in the frequency range $f \in [1.215; 1.350]$ Ghz;

- S-band in the frequency range $f \in [2.7; 3.1]$ GHz.

Commercial systems work on the operational frequency band $f \in [2.7; 2.9]$ GHz.

Transmitted power depends on the number of transmitting modules in the feeder, that are usually composed by more than one horn antennas, and on the range (typically measured in naval miles [nm]) that the radar has to cover. Taking as example the ASR-12 produced by Indra, the peak power is 19.2 kW for a maximum detection range from 60 to 80 naval miles.

The dimensions of an ASCSignal™PSR are reported. In particular the parabolic reflector has surface dimensions of $4.05\,m \times 4.20\,m \times 5.06\,m$ (l × w × h) and a net weight of 2640 kg. The rotating pedestal has a net weight of 4560 kg with dimensions $2.3\,m \times 2.3\,m \times 2.4\,m$ (l × w × h). The power consumption of the pedestal is of about 10KW that is about the 50 % of the power trasmitted by the antenna.

Hence finding a structure that permits the scanning of the entire space without mechanical steering is important not only because in that way it is possible to scan different angular sectors simultaneously but because removing the rotating pedestal is also convenient from a power consumption point of view.

Figure 4: EASAT EP1643 rotating Pedestal

*Fig.*4 shows an example of real rotating pedestal, the EASAT EP1643.

Antenna System	
Frequency Band [GHz]	S-band $f \in [2.7; 2.9]$
Elevation Range [deg]	40
Detection Range [nm]	$[60; 80]$
Peak Power [kW]	$[20; 50]$
Feeding Techniques	Horn Antennas
Approximative Dimensions ($l \times w \times h$) [m]	$4.00 \times 4.50 \times 5.00$
Weight [kg]	$[2500; 2700]$
rotating Pedestal	
Power Consumption [kW]	$[10; 12]$
Approximative Dimensions ($l \times w \times h$) [m]	$2 \times 2 \times 2.5$
Weight [kg]	4500

Table I: Typical PSR approximative characteristics resume

*Tab.*I report a brief resume of principal PSR antenna system characteristics. The values have been approximated taking as examples systems .

2.2 Proposed ATC System
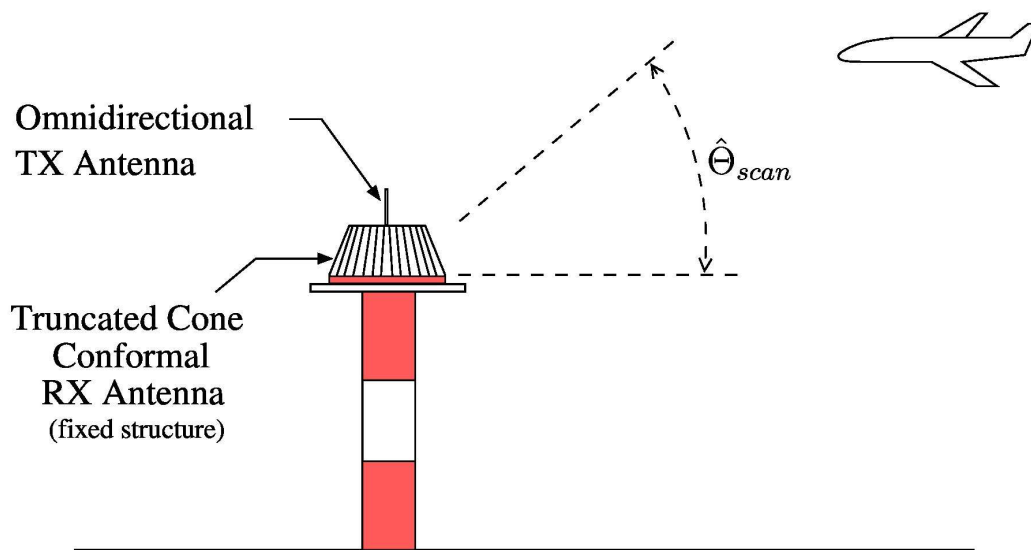
Figure 5: Proposed ATC Scenario

The proposed ATC scenario is shown in *Fig.5*. In particular the system is fixed and is composed by an omnidirectional transmitting antenna and the Truncated Cone Conformal Phased Array receiving antenna.

The transmitting antenna is not described in this document because it could be implemented by means a simple monopole or dipole antenna, or an helical antenna in normal mode. Hence its design is based on well known formulas that can be found.

As mentioned before in *Section 2.1*, the design of a fixed structure that permits the radiation at 360 degrees is quite unusual and surely innovative in the field of civil ATC applications.

In order to substitute the rotating pedestal typical of today's commercial PSRs , the choice of a geometry that permits a similar behavior to the rotating one was necessary so the Truncated Cone structure has been choosen as the one that permits the best approximation.

In detail the receiving antenna is not a complete conformal phased array but a collection of linear array assuming a conformal shape. In this way it is possible to select precisely one array or a set of them in order to perform radiation in the wanted direction. Then switching on and off particular linear arrays a 360 degrees ratiation is possible.

In addition to the radiation all around the structure a beam steering in elevation is achievable exploiting the key feature of phased array. Changing excitations phases in fact permits to steer the beam pattern in order to cover an angular range in elevation similar to the one of commercial reference systems as shown in *Fig.*5. The resulting beam pattern in elevation will not be as the reference one but, considering a singular linear array or a set of them, will be a single beam steered along multiple steering angles in the elevation range and then steered in azimut to scan the space all around the antenna.

As reported in *Section 4.2*, *5.7* and *5.8* it is possible to divide the structure in indipendent sectros each of them characterized by the radiating behavior described before. In this way multiple sectors of space can be scanned
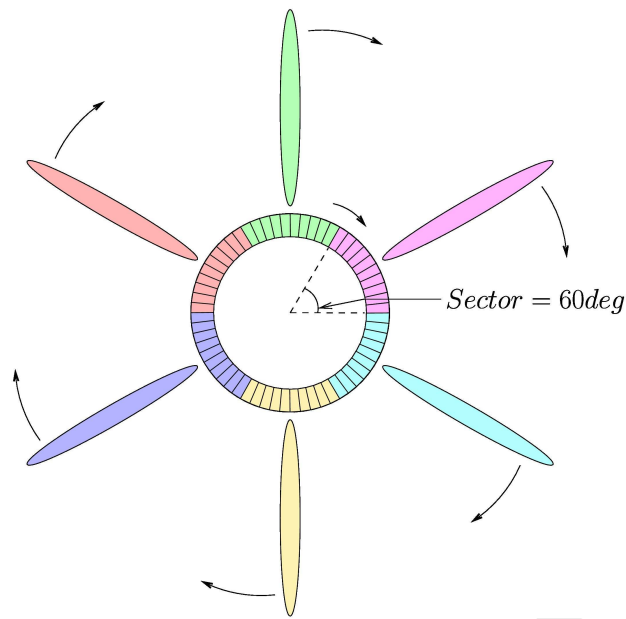
Figure 6: Multiple beam radiation, conceptual behavior - top view

perfoming a rotation of the selected linear arrays simply turning them on and off.

A conceptual representation of this behavior is in *Fig.*6. This scheme represent the top view of the structure where for examples has been choosen 60 degrees sectors. Number of linear arrays per sector and shape of beams are examples. Size of sectors and consequently number of concurrent beams will results from a trade off between desired directivity and half power beamwidth in azimut ($HPBW_{az}$) because directivity ($HPBW_{az}$) will increase (decrease) as size of sector increase that means increasing the number of linear arrays per active sector.

Proposed architecture will have also the advantage to be more robust to avverse weather conditions with respect to parabolic reflector antenna systems due to its particular shape.

2.3 Truncated Cone Antenna Geometry and Architecture
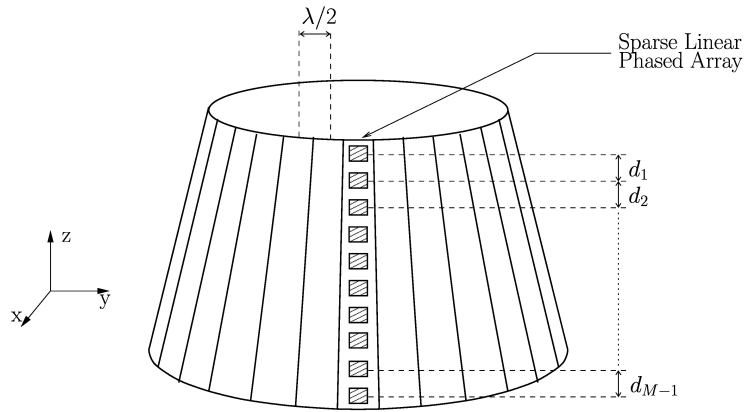
Figure 7: Truncated Cone Radar Architecture conceptual scheme

Proposed antenna geometry is shown in *Fig.*7. As mentioned before the structure is composed by a number C of linear array disposed over a truncated cone structure, each one composed by M elements. The spacing between arrays is of $0.5\,\lambda$ on the upper base. In the conceptual scheme is shown only one linear array to simplify the figure.
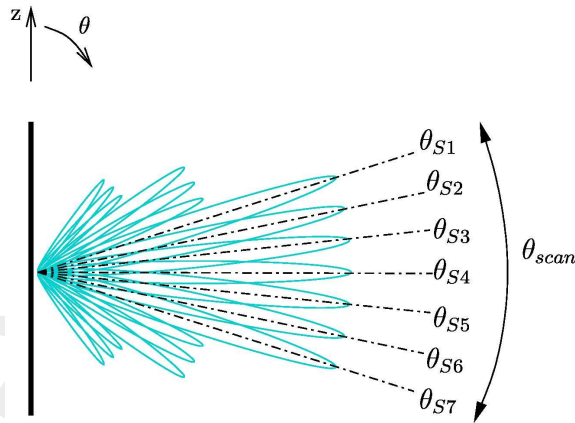
Figure 8: Beam steering of a "vertical" linear array

The detailed designing procedure is reported below.

Starting from a reference *Uniformly Spaced Linear Array* (*USLA*) with interelement spacing of 0.5λ, it has been synthesized in order to obtain a set of excitations that permits a beam steering to cover an angular region $\hat{\Theta}_{scan}$ as shown in *Fig.* 8, that has been fixed at value $\hat{\Theta}_{scan} = 40$, similarly to the reference commercial systems reported in *Section 2.2*. The number of elements M for the reference USLA has been chosen in order to cover, with I steered beams, an angular region equal to $\hat{\Theta}_{scan}$ as sum of the HPBWs of all considered beams.

At this point the reference USLA had to be optimized in order to reduce the number of elements. To do that, has been used the Multi-task Bayesian Compressive Sensing (*MT-BCS*).

MT-BCS sybthesis procedure gives as output array elements exitations (amplitudes and phases) of a Sparse Linear Array characterized by a power pattern very similar to the reference input one but with number of
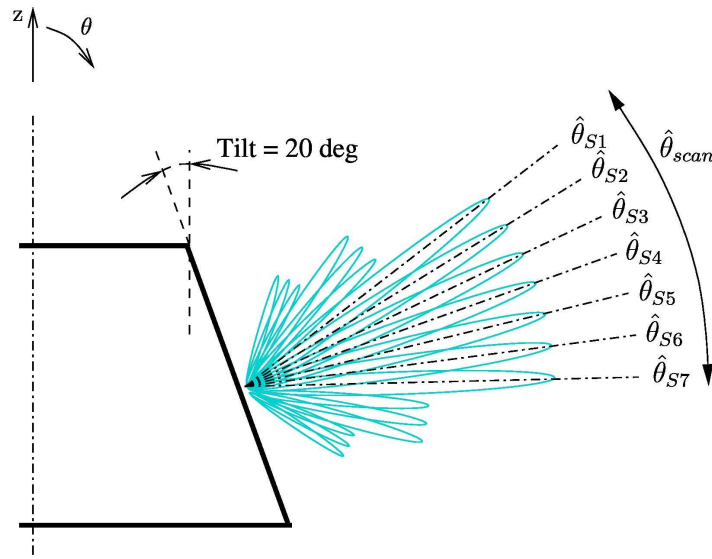
Figure 9: Beam steering of a linear array on Truncated Cone structure

elements less than it. Hence output linear array is no longer Unoformly Spaced but with inter-element spacing not constant maintaining the overall spatial dimension unchanged.

Then the resulting sparse linear array has been used to compose the entire Truncated Cone structure reproducing it C times.

Thanks to the shape of the chosen geometry, it is possible to exploit two peculiar features:

- circular symmetry permits the radiation in the space all around the antenna without the mechanical rotation typical of todays commercial systems;

- slope of lateral surface (*Tilt* from now on) permits the steering of all beams of an additional angle in elevation equal to the value of the slope.

In detail, as shown in *Fig.* 9, tilting linear arrays has as result that the radiation is not towards the ground, as in case of the beam steered at θ_{S7} in "vertical" case (*Fig.*8), but parallel to it as in case of beam steered at $\hat{\theta}_{S7}$ in truncated cone case (*Fig.* 9).

The slope of lateral surface has been set at value $Tilt = 20$.

Proposed system is designed to be fed by a *Fully Digital* beamforming network which conceptual scheme is shown in *Fig.*10. For each element of the singular linear array only an ADC block is needed instead of a phase shifter and an amplifier as in analog beamforming networks,. In *Fig.11* is shown the ADC block scheme of the n-th radiating element.
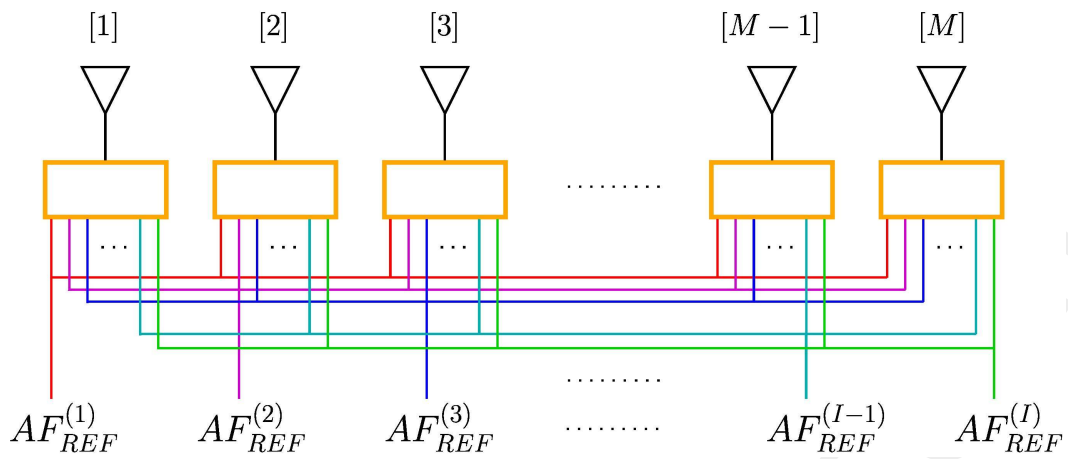
Figure 10: Fully Digital Beamforming Network scheme

The ADC block is composed by a bandpass filter and an ADC with a number of input ports equal to the number of reference patterns. Amplifiers and phase shifters are "virtual": infact amplitudes and phases are numerical variables obtained as output of the MT-BCS synthesis procedure. In this way the beam steering could be implemented by means of code subrutines permitting a consistent improvement on reliability and reconfigurability with respect to analog systems.
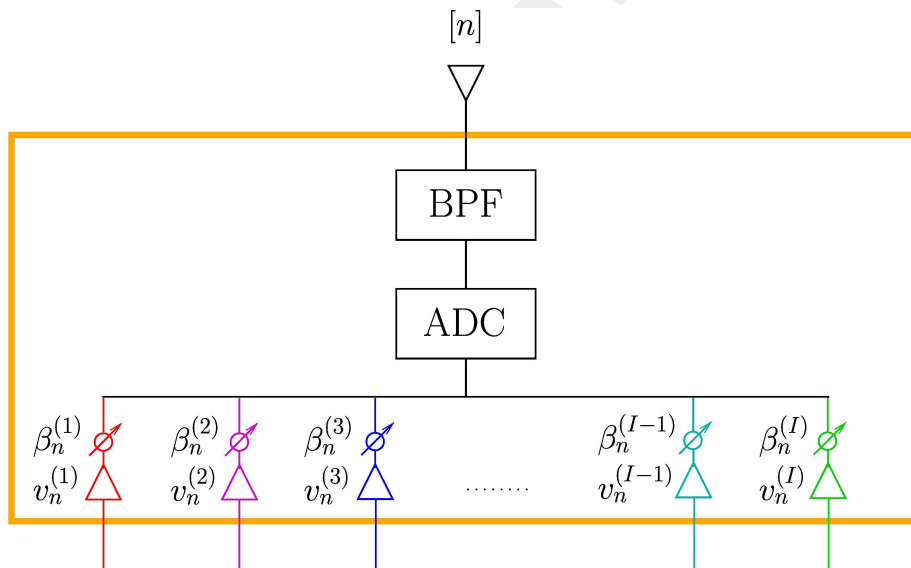
Figure 11: ADC conceptual scheme

3 Mathematical formulation

3.1 MT-BCS Synthesis Procedure

The synthesis procedure is based on a pattern matching problem represented by the following formula

$$\sum_{k=1}^{K} \left| AF_{REF}^{(i)}(u_k) - \sum_{m=1}^{M} v_m^{(i)} e^{(j2\pi l_m u_k)} \right|^2 \leq \epsilon \qquad i = 1, \ldots, I. \tag{1}$$

In particular the problem is to find the minimum number of elements M that satisfy the equation above in order to matching all the I reference patterns. The differnece between the procedure reported The pattern matching has to be verified on all the reference power patterns considered and not on only one.

Each reference pattern is sampled in K sampling points, called *Pattern Samples*. For each point is computed the difference between the reference pattern value and the value of the pattern generated by a sparse array composed by M elements selected over a number of N arbitrary positions, called *Aperture Samples*, in order to satisfy the threshold value ϵ that represent how much the two patterns are similar. The range in which *Aperture Samples* are selected has the same dimensions of the reference array elements positions space. In practice the reference array elements positions space is oversampled with N samples.

In (1) $AF_{REF}^{(i)}(u_k) \in \mathbb{C}$ is the k-th sample of the i-th reference pattern at the angle $u_k \in [-1, 1]$, $v_m^{(i)} \in \mathbb{C}$ are the complex weights of the sparse array for the generation of the i-th matching pattern and l_m its elements positions expressed in wavelengths. As stated, the M elements positions are selected over a number N of arbitrary location d_n ($n = 1, ..., N$) with $N \gg M$ in order to satisfy the sparsening of the resulting array. Hence it is possible to define the sparse weights vector as $\mathbf{w} = \{w_n; n = 1, ..., N\}$ where

$$w_n = \begin{cases} v_m & if \ d_n = l_m \\ 0 & otherwise. \end{cases} \tag{2}$$

Exploiting the definition of the sparse weight vector $\mathbf{w}$, it is possible to write (1), as

$$\mathbf{AF}_{REF}^{(i)} - [\mathbf{\Phi}]\mathbf{w}^{(i)} = \mathcal{E}^{(i)} \qquad i = 1, \ldots, I \tag{3}$$

where: $\mathbf{AF}_{REF}^{(i)}$ is the observation vector that contains the i-th reference pattern samples values, $[\mathbf{\Phi}]$ is the exponential matrix of the system containing the exponential terms of the array factor that depend on element positions, $\mathbf{w}^{(i)}$ is the i-th sparse weights vector and $\mathcal{E}^{(i)}$ is the i-th error vector with zero mean value and variance σ^2.

In particular

$$\mathbf{AF}_{REF}^{(i)} = \left\{ AF_{REF}^{(i)}(u_k) \in \mathbb{C}; k = 1, \ldots, K \right\} \tag{4}$$

$$\mathbf{\Phi} = \begin{bmatrix} e^{\left(\frac{j\,2\pi\,d_1\,u_1}{\lambda}\right)} & \cdots & e^{\left(\frac{j\,2\pi\,d_N\,u_1}{\lambda}\right)} \\ \vdots & \ddots & \vdots \\ e^{\left(\frac{j\,2\pi\,d_1\,u_K}{\lambda}\right)} & \cdots & e^{\left(\frac{j\,2\pi\,d_N\,u_K}{\lambda}\right)} \end{bmatrix} \tag{5}$$

$$\mathbf{w}^{(i)} = \left\{ w_n^{(i)};\, n = 1, \ldots, N \right\}. \tag{6}$$

With MT-BCS it is possible to overcome the limit of BCS of addressing only real valued problems. In detail MT-BCS exploits the definition of two *fictitious weights vectors*, $\mathbf{w}_{Re}$ and $\mathbf{w}_{Im}$, respectively composed by real and imaginary part values of weights vector $\mathbf{w}$.

The two vectors are defined as:

$$\begin{cases} \mathbf{w}_{Re} \triangleq \mathcal{R}\{\mathbf{w}\} \\ \mathbf{w}_{Im} \triangleq \mathcal{I}\{\mathbf{w}\} \end{cases} \qquad \mathbf{w}_{Re},\, \mathbf{w}_{Im} \in \mathbb{R}^N. \tag{7}$$

Since $\mathbf{AF}_{REF}^{(i)} \in \mathbb{C}$ it is possible to divide the synthesis problem in terms of its real and imaginary part using vector definitions at (7). The formula at (3) become

$$\begin{cases} \hat{\mathbf{AF}}_{Re}^{(i)} - \hat{\mathbf{\Phi}}\mathbf{w}_{Re}^{(i)} = \hat{\mathcal{E}}_{Re}^{(i)} \\ \hat{\mathbf{AF}}_{Im}^{(i)} - \hat{\mathbf{\Phi}}\mathbf{w}_{Im}^{(i)} = \hat{\mathcal{E}}_{Im}^{(i)}. \end{cases} \tag{8}$$

where $\hat{\mathbf{AF}}_{Re}^{(i)} = \left[\mathcal{R}\{\mathbf{AF}_{Re}^{(i)}\}, \mathcal{I}\{\mathbf{AF}_{Re}^{(i)}\}\right]$, $\hat{\mathbf{AF}}_{Im}^{(i)} = \left[\mathcal{R}\{\mathbf{AF}_{Im}^{(i)}\}, \mathcal{I}\{\mathbf{AF}_{Im}^{(i)}\}\right]$ $\left(\hat{\mathbf{AF}}_{Re}, \hat{\mathbf{AF}}_{Im} \in \mathbb{R}^{2K}\right)$ with $i = 1, \ldots, I$, $\hat{\mathbf{\Phi}} \triangleq [\mathcal{R}\{\mathbf{\Phi}\}, \mathcal{I}\{\mathbf{\Phi}\}]$, and $\hat{\mathcal{E}}_{Re}^{(i)}, \hat{\mathcal{E}}_{Im}^{(i)} \in \mathbb{R}^{2K}$ with $i = 1, \ldots, I$ are the complex Gaussian error vectors with zero-mean and variance $\sigma^2/2$. Finally it is possible to write $\mathbf{AF}_{REF}^{(i)}$ as

$$\mathbf{AF}_{REF}^{(i)} = \mathbf{AF}_{Re}^{(i)} + i\mathbf{AF}_{Im}^{(i)} \qquad i = 1, \ldots, I \tag{9}$$

since $\mathbf{AF}_{Re}^{(i)}, \mathbf{AF}_{Im}^{(i)} \in \mathbb{C}^K$.

The MT-BCS real-valued synthesis problem could be formulated as MT-BCS *"Deterministic" Synthesis Problem*, that is find the weights vectors $\mathbf{w}_{Re}^{(i)}$ and $\mathbf{w}_{Im}^{(i)}$ ($\mathbf{w}_{Re}^{(i)}, \mathbf{w}_{Im}^{(i)} \in \mathbb{R}^N$) with minimum l_0-norm so that (8) is satisfied.

Previous definition could be recast as MT-BCS *"Probabilistic" Synthesis Problem* that is find the weights vectors $\mathbf{w}_{Re}^{(i)}$ and $\mathbf{w}_{Im}^{(i)}$ ($\mathbf{w}_{Re}^{(i)}, \mathbf{w}_{Im}^{(i)} \in \mathbb{R}^N$) with minimum l_0-norm that satisfy the following expression

$$\begin{cases} \mathbf{w}_{Re}^{MT-BCS\,(i)} = \arg\left[\max_{\mathbf{w}_{Re}^{(i)}} \mathcal{P}\left(\mathbf{w}_{Re}^{(i)} \mid \hat{\mathbf{AF}}_{Re}^{(i)}\right)\right] \\ \mathbf{w}_{Im}^{MT-BCS\,(i)} = \arg\left[\max_{\mathbf{w}_{Im}^{(i)}} \mathcal{P}\left(\mathbf{w}_{Im}^{(i)} \mid \hat{\mathbf{AF}}_{Im}^{(i)}\right)\right] \end{cases} \qquad i = 1, \ldots, I. \tag{10}$$

The solution of (10) is real-valued and is given by

$$
\begin{cases}
\mathbf{w}_{Re}^{MT-BCS\,(i)} = \left(diag\left(\hat{\mathbf{a}}^{MT-BCS}\right) + \hat{\boldsymbol{\Phi}}^T\hat{\boldsymbol{\Phi}}\right)^{-1}\hat{\boldsymbol{\Phi}}^T\mathbf{A}\hat{\mathbf{F}}_{Re}^{(i)} \\
\mathbf{w}_{Im}^{MT-BCS\,(i)} = \left(diag\left(\hat{\mathbf{a}}^{MT-BCS}\right) + \hat{\boldsymbol{\Phi}}^T\hat{\boldsymbol{\Phi}}\right)^{-1}\hat{\boldsymbol{\Phi}}^T\mathbf{A}\hat{\mathbf{F}}_{Im}^{(i)}
\end{cases}
\qquad i = 1, \ldots, I
\tag{11}
$$

that it is possible to write shortly as

$$
\mathbf{w}_S^{MT-BCS} = \left(diag\left(\hat{\mathbf{a}}^{MT-BCS}\right) + \hat{\boldsymbol{\Phi}}^T\hat{\boldsymbol{\Phi}}\right)^{-1}\hat{\boldsymbol{\Phi}}^T\mathbf{A}\hat{\mathbf{F}}_S \qquad S \in \left\{R^{(1)}, \ldots, R^{(I)}, I^{(1)}, \ldots, I^{(I)}\right\}.
\tag{12}
$$

where $\hat{\mathbf{a}}$ is defined as the *Shared Hyperparameters vector.*

In order to solve (10) it is necessary to define the conditional probability $\mathcal{P}\left(\mathbf{w}_S | \mathbf{A}\hat{\mathbf{F}}_S\right)$. Exploiting Bayes theorem, this probability can be defined as

$$
\mathcal{P}\left(\mathbf{w}_S | \mathbf{A}\hat{\mathbf{F}}_S\right) \triangleq \frac{\mathcal{P}(\mathbf{A}\hat{\mathbf{F}}_S \mid \mathbf{w}_S)\mathcal{P}(\mathbf{w}_S)}{\mathcal{P}(\mathbf{A}\hat{\mathbf{F}}_S)}
\tag{13}
$$

where $\mathcal{P}(\mathbf{w}_S)$ and $\mathcal{P}(\mathbf{A}\hat{\mathbf{F}}_S)$ are the a priori probabilities of $\mathbf{w}_S^{(i)}$ and $\mathbf{A}\hat{\mathbf{F}}_S$.

Prior $\mathcal{P}(\mathbf{w}_S)$ is useful to define not only the sparsity of the weights vectors but also the correlation between them, in fact for its computation is needed the introduction of the shared hyperparameters vector $\hat{\mathbf{a}} = \{a_n; 1, \ldots, N\}, \hat{\mathbf{a}} \in \mathbb{R}^N$. The hyperparameters vector is shared among all the computational tasks. For the single pattern matching case ($I = 1$), the number of parallel task needed to solve the synthesis problem is $T = 2$ (one task for the real part and one for the imaginary part of the weights vector). The proposed work is based instead on I patterns matching that means a number of $T = 2I$ tasks. In paticular

$$
\mathcal{P}(\mathbf{w}_S) = \int \mathcal{P}(\mathbf{w}_S \mid \hat{\mathbf{a}}, \hat{\sigma}^2)\mathcal{P}(\hat{\mathbf{a}})\mathcal{P}(\hat{\sigma}^2)\,d\hat{\mathbf{a}}d\hat{\sigma}^2.
\tag{14}
$$

Now, using (13) and (14) it is possible to write (10) as

$$
\mathbf{w}_S^{MT-BCS} = \arg\left\{\max_{\mathbf{w}_S}\left[\int \frac{\mathcal{P}(\mathbf{w}_S \mid \hat{\mathbf{a}}, \hat{\sigma}^2)\mathcal{P}(\mathbf{A}\hat{\mathbf{F}}_S \mid \mathbf{w}_S)\mathcal{P}(\hat{\mathbf{a}})\mathcal{P}(\hat{\sigma}^2)}{\mathcal{P}(\mathbf{A}\hat{\mathbf{F}}_S)}\,d\hat{\mathbf{a}}d\hat{\sigma}^2\right]\right\}
$$

$$
= \arg\left\{\max_{\mathbf{w}_S}\left[\int \mathcal{P}(\mathbf{w}_S \mid \mathbf{A}\hat{\mathbf{F}}_S, \hat{\mathbf{a}})\mathcal{P}(\hat{\mathbf{a}} \mid \mathbf{A}\hat{\mathbf{F}}_S)\,d\hat{\mathbf{a}}\right]\right\}
\tag{15}
$$

where $\mathcal{P}(\mathbf{w}_S \mid \mathbf{A}\hat{\mathbf{F}}_S, \hat{\mathbf{a}})$ is defined as

$$
\mathcal{P}(\mathbf{w}_S \mid \mathbf{A}\hat{\mathbf{F}}_S, \hat{\mathbf{a}}) = \left(\int_0^\infty t^{\gamma_a + N/2 - 1}e^{-t}dt\right)\frac{\left[1 + \frac{1}{2\gamma_b}\left(\mathbf{w}_S - \hat{\mu}_S\right)\right]^{-(\gamma_a + N/2)}}{\left(\int_0^\infty t^{\gamma_a - 1}e^{-t}dt\right)(2\pi\gamma_2)^{N/2}\sqrt{\left|\hat{\Sigma}\right|}}
\tag{16}
$$

with $\hat{\mu}_S \triangleq \hat{\Sigma}\hat{\Phi}^T \mathbf{A}\hat{\mathbf{F}}_S$ and $\hat{\Sigma} \triangleq \left(diag(\hat{\mathbf{a}}) + \hat{\Phi}^T\hat{\Phi}\right)^{-1}$.

For $\mathcal{P}(\hat{\mathbf{a}} \mid \mathbf{A}\hat{\mathbf{F}}_S)$ does not exist a closed form solution but approximating it to

$$\mathcal{P}(\hat{\mathbf{a}} \mid \mathbf{A}\hat{\mathbf{F}}_S) \propto \mathcal{P}(\mathbf{A}\hat{\mathbf{F}}_S \mid \hat{\mathbf{a}})\mathcal{P}(\hat{\mathbf{a}}). \tag{17}$$

it is possible to compute its mode over all the $2I$ tasks ($S \in \left\{R^{(1)}, \ldots, R^{(I)}, I^{(1)}, \ldots, I^{(I)}\right\}$) obtaining

$$\hat{\mathbf{a}}^{MT-BCS} = \arg\max_{\hat{\mathbf{a}}}\{\mathcal{L}^{MT-BCS}(\hat{\mathbf{a}})\} \tag{18}$$

where $\mathcal{L}^{MT-BCS}(\hat{\mathbf{a}})$, defined as

$$\mathcal{L}^{MT-BCS}(\hat{\mathbf{a}}) = \frac{1}{2}\sum_S \left\{\log\left(\left|I + \hat{\Phi}\left[diag(\hat{\mathbf{a}})\right]^{-1}\hat{\Phi}^T\right|\right) + (N + 2\gamma_a)\log\left[\mathbf{A}\hat{\mathbf{F}}_S^T\left(I + \hat{\Phi}\left[diag(\hat{\mathbf{a}})\right]^{-1}\hat{\Phi}^T\right)\mathbf{A}\hat{\mathbf{F}}_S + 2\gamma_b\right]\right\} \tag{19}$$

is the logarithm of the MT-BCS marginal likelihood.

Finally, giving that (16) is charaterized by a multivariate *Student-t* distribution which mode is equal to its mean value ($\hat{\mu}_S$) and that $\mathcal{P}(\hat{\mathbf{a}} \mid \mathbf{A}\hat{\mathbf{F}}_S) \approx \delta\left(\hat{\mathbf{a}} - \hat{\mathbf{a}}^{MT-BCS}\right)$ it is possible to write

$$\mathbf{w}_S^{MT-BCS} = \arg\left\{\max_{\mathbf{w}_S}\left[\int \mathcal{P}(\mathbf{w}_S \mid \mathbf{A}\hat{\mathbf{F}}_S, \hat{\mathbf{a}})\delta\left(\hat{\mathbf{a}} - \hat{\mathbf{a}}^{MT-BCS}\right)d\hat{\mathbf{a}}\right]\right\}$$

$$= \arg\left\{\max_{\mathbf{w}_S}\left[\mathcal{P}(\mathbf{w}_S \mid \mathbf{A}\hat{\mathbf{F}}_S, \hat{\mathbf{a}}^{MT-BCS})\right]\right\}$$

Figure #: elem

$$= \hat{\mu}_S = \left(diag\left(\hat{\mathbf{a}}^{MT-BCS}\right) + \hat{\Phi}^T\hat{\Phi}\right)^{-1}\hat{\Phi}^T\mathbf{A}\hat{\mathbf{F}}_S \qquad S \in \left\{R^{(1)}, \ldots, R^{(I)}, I^{(1)}, \ldots, I^{(I)}\right\} \tag{20}$$

3.2 MT-BCS error computation

In order to define the quality of the power patterns generated by the sparse array obtainded as output of the MT-BCS synthesis procedure it is necessary to compute the error between the reference power patterns and the "MT-BCS" ones. The error has been computed for each pair of reference and MT-BCS power pattern and the results has been mediate in order to compute the total error of the entire synthesis procedure.

In detail the formulas used to estimate the errors are

$$err_i = \sum_{k=1}^{K} \left| AF_{REF}^{(i)}(k) - AF_{MT-BCS}^{(i)}(k) \right| \tag{21}$$

$$\xi = \frac{1}{I} \sum_{i=1}^{I} err_i \tag{22}$$

where err_i is the error between i-th reference pattern and i-th MT-BCS output pattern, with I total number of reference patterns.

More information on the topics of this document can be found in the following list of references.

References

[1] P. Rocca, G. Oliveri, R. J. Mailloux, and A. Massa, "Unconventional phased array architectures and design Methodologies - A review," *Proceedings of the IEEE - Special Issue on 'Phased Array Technologies'*, Invited Paper, vol. 104, no. 3, pp. 544-560, March 2016.

[2] A. Massa, P. Rocca, and G. Oliveri, "Compressive sensing in electromagnetics - A review," *IEEE Antennas Propag. Mag.*, pp. 224-238, vol. 57, no. 1, Feb. 2015.

[3] F. Zardi, G. Oliveri, M. Salucci, and A. Massa, "Minimum-complexity failure correction in linear arrays via compressive processing," *IEEE Trans. Antennas Propag.*, vol. 69, no. 8, pp. 4504-4516, Aug. 2021.

[4] N. Anselmi, G. Gottardi, G. Oliveri, and A. Massa, "A total-variation sparseness-promoting method for the synthesis of contiguously clustered linear architectures" *IEEE Trans. Antennas Propag.*, vol. 67, no. 7, pp. 4589-4601, Jul. 2019.

[5] M. Salucci, A. Gelmini, G. Oliveri, and A. Massa, "Planar arrays diagnosis by means of an advanced Bayesian compressive processing," *IEEE Tran. Antennas Propag.*, vol. 66, no. 11, pp. 5892-5906, Nov. 2018.

[6] L. Poli, G. Oliveri, P. Rocca, M. Salucci, and A. Massa, "Long-Distance WPT Unconventional Arrays Synthesis" *J. Electromagn. Waves Appl.*, vol. 31, no. 14, pp. 1399-1420, Jul. 2017.

[7] G. Oliveri, M. Salucci, and A. Massa, "Synthesis of modular contiguously clustered linear arrays through a sparseness-regularized solver," *IEEE Trans. Antennas Propag.*, vol. 64, no. 10, pp. 4277-4287, Oct. 2016.

[8] M. Carlin, G. Oliveri, and A. Massa, "Hybrid BCS-deterministic approach for sparse concentric ring isophoric arrays," *IEEE Trans. Antennas Propag.*, vol. 63, no. 1, pp. 378-383, Jan. 2015.

[9] G. Oliveri, E. T. Bekele, F. Robol, and A. Massa, "Sparsening conformal arrays through a versatile BCS-based method," *IEEE Trans. Antennas Propag.*, vol. 62, no. 4, pp. 1681-1689, Apr. 2014.

[10] F. Viani, G. Oliveri, and A. Massa, "Compressive sensing pattern matching techniques for synthesizing planar sparse arrays," *IEEE Trans. Antennas Propag.*, vol. 61, no. 9, pp. 4577-4587, Sept. 2013.

[11] G. Oliveri, P. Rocca, and A. Massa, "Reliable diagnosis of large linear arrays - A Bayesian Compressive Sensing approach," *IEEE Trans. Antennas Propag.*, vol. 60, no. 10, pp. 4627-4636, Oct. 2012.

[12] G. Oliveri, M. Carlin, and A. Massa, "Complex-weight sparse linear array synthesis by Bayesian Compressive Sampling," *IEEE Trans. Antennas Propag.*, vol. 60, no. 5, pp. 2309-2326, May 2012.

[13] G. Oliveri and A. Massa, "Bayesian compressive sampling for pattern synthesis with maximally sparse non-uniform linear arrays," *IEEE Trans. Antennas Propag.*, vol. 59, no. 2, pp. 467-481, Feb. 2011.

[14] A. Benoni, P. Rocca, N. Anselmi, and A. Massa, "Hilbert-ordering based clustering of complex-excitations linear arrays," *IEEE Trans. Antennas Propag.*, vol. 70, no. 8, pp. 6751-6762, Aug. 2022.

[15] P. Rocca, L. Poli, N. Anselmi, and A. Massa, "Nested optimization for the synthesis of asymmetric shaped beam patterns in sub-arrayed linear antenna arrays," *IEEE Trans. Antennas Propag.*, vol. 70, no. 5, pp. 3385 - 3397, May 2022.

[16] P. Rocca, L. Poli, A. Polo, and A. Massa, "Optimal excitation matching strategy for sub-arrayed phased linear arrays generating arbitrary shaped beams," *IEEE Trans. Antennas Propag.*, vol. 68, no. 6, pp. 4638-4647, Jun. 2020.

[17] G. Oliveri, G. Gottardi and A. Massa, "A new meta-paradigm for the synthesis of antenna arrays for future wireless communications," *IEEE Trans. Antennas Propag.*, vol. 67, no. 6, pp. 3774-3788, Jun. 2019.

[18] P. Rocca, M. H. Hannan, L. Poli, N. Anselmi, and A. Massa, "Optimal phase-matching strategy for beam scanning of sub-arrayed phased arrays," *IEEE Trans. Antennas Propag.*, vol. 67, no. 2, pp. 951-959, Feb. 2019.

[19] N. Anselmi, P. Rocca, M. Salucci, and A. Massa, "Contiguous phase-clustering in multibeam-on-receive scanning arrays" *IEEE Trans. Antennas Propag.*, vol. 66, no. 11, pp. 5879-5891, Nov. 2018.

[20] L. Poli, G. Oliveri, P. Rocca, M. Salucci, and A. Massa, "Long-distance WPT unconventional arrays synthesis" *J. Electromagn. Waves Appl.*, vol. 31, no. 14, pp. 1399-1420, Jul. 2017.

[21] G. Gottardi, L. Poli, P. Rocca, A. Montanari, A. Aprile, and A. Massa, "Optimal monopulse beamforming for side-looking airborne radars," *IEEE Antennas Wirel. Propag. Lett.*, vol. 16, pp. 1221-1224, 2017.

[22] P. Rocca, M. D'Urso, and L. Poli, "Advanced strategy for large antenna array design with subarray-only amplitude and phase contr," *IEEE Antennas and Wirel. Propag. Lett.*, vol. 13, pp. 91-94, 2014.

[23] L. Manica, P. Rocca, G. Oliveri, and A. Massa, "Synthesis of multi-beam sub-arrayed antennas through an excitation matching strategy," *IEEE Trans. Antennas Propag.*, vol. 59, no. 2, pp. 482-492, Feb. 2011.

[24] M. Salucci, G. Oliveri, and A. Massa, "An innovative inverse source approach for the feasibility-driven design of reflectarrays," *IEEE Trans. Antennas Propag.*, vol. 70, no. 7, pp. 5468-5480, July 2022.

[25] L. T. P. Bui, N. Anselmi, T. Isernia, P. Rocca, and A. F. Morabito, "On bandwidth maximization of fixed-geometry arrays through convex programming," *J. Electromagn. Waves Appl.*, vol. 34, no. 5, pp. 581-600, 2020.

[26] N. Anselmi, L. Poli, P. Rocca, and A. Massa, "Design of simplified array layouts for preliminary experimental testing and validation of large AESAs," *IEEE Trans. Antennas Propag.*, vol. 66, no. 12, pp. 6906-6920, Dec. 2018.

[27] G. Oliveri and T. Moriyama, "Hybrid PS-CP technique for the synthesis of n-uniform linear arrays with maximum directivity" *J. Electromagn. Waves Appl.*, vol. 29, no. 1, pp. 113-123, Jan. 2015.

[28] P. Rocca and A. Morabito, "Optimal synthesis of reconfigurable planar arrays with simplified architectures for monopulse radar applications" *IEEE Trans. Antennas Propag.*, vol. 63, no. 3, pp. 1048-1058, Mar. 2015.

[29] A. F. Morabito and P. Rocca, "Reducing the number of elements in phase-only reconfigurable arrays generating sum and difference patterns," *IEEE Antennas Wireless Propag. Lett.*, vol. 14, pp. 1338-1341, 2015.

[30] P. Rocca, N. Anselmi, and A. Massa, "Optimal synthesis of robust beamformer weights exploiting interval analysis and convex optimization," *IEEE Trans. Antennas Propag.*, vol. 62, no. 7, pp. 3603-3612, Jul. 2014.

[31] G. Oliveri, G. Gottardi, M. A. Hannan, N. Anselmi, and L. Poli, "Autocorrelation-driven synthesis of antenna arrays - The case of DS-based planar isophoric thinned arrays," *IEEE Trans. Antennas Propag.*, vol. 68, no. 4, pp. 2895-2910, Apr. 2020.

[32] M. Salucci, G. Gottardi, N. Anselmi, and G. Oliveri, "Planar thinned array design by hybrid analytical-stochastic optimization," *IET Microw. Antennas Propag.*, vol. 11, no. 13, pp. 1841-1845, Oct. 2017

[33] T. Moriyama, E. Giarola, M. Salucci, and G. Oliveri, "On the radiation properties of ADS-thinned dipole arrays" *IEICE Electronics Express*, vol. 11, no. 16, pp. 1-10, Aug. 2014.

[34] G. Oliveri, F. Viani, and A. Massa, "Synthesis of linear multi-beam arrays through hierarchical ADS-based interleaving," *IET Microw. Antennas Propag.*, vol. 8, no. 10, pp. 794-808, Jul. 2014.

[35] D. Sartori, G. Oliveri, L. Manica, and A. Massa, "Hybrid Design of non-regular linear arrays with accurate control of the pattern sidelobes," *IEEE Trans. Antennas Propag.*, vol. 61, no. 12, pp. 6237-6242, Dec. 2013.